Check for updates

AGU100 ADVANCING EARTH AND SPACE SCIENCE

Water Resources Research

RESEARCH ARTICLE
10.1029/2019WR025686

An Adjoint Sensitivity Model for Steady-State Sequentially Coupled Radionuclide Transport in Porous Media

Mohamed Hayek[1], **Banda S. RamaRao**[2], **and Marsh Lavenue**[2]

[1]INTERA Incorporated, Wettingen, Switzerland, [2]INTERA Incorporated, Austin, TX, USA

Key Points:
- A full mathematical/numerical adjoint sensitivity approach for steady-state sequentially coupled radionuclide transport in heterogeneous media is presented
- Analytical expressions including adjoint state functions and sensitivity coefficients are derived in closed forms for the homogeneous case
- A derivative-based global sensitivity method coupled with the adjoint approach is presented and applied to a real field case

Supporting Information:
- Supporting Information S1

Correspondence to:
M. Hayek,
mhayek@intera.com;
mohamed.hayek@gmail.com

Citation:
Hayek, M., RamaRao, B. S., & Lavenue, M. (2019). An adjoint sensitivity model for steady-state sequentially coupled radionuclide transport in porous media. *Water Resources Research*, *55*, 8800–8820. https://doi.org/10.1029/2019WR025686

Received 29 JUL 2018
Accepted 6 SEP 2019
Accepted article online 10 SEP 2019
Published online 11 NOV 2019

This article was corrected on 17 JUN 2020. See the end of the full text for details.

Abstract This work presents an efficient mathematical/numerical model to compute the sensitivity coefficients of a predefined performance measure to model parameters for one-dimensional steady-state sequentially coupled radionuclide transport in a finite heterogeneous porous medium. The model is based on the adjoint sensitivity approach that offers an elegant and computationally efficient alternative way to compute the sensitivity coefficients. The transport parameters include the radionuclide retardation factors due to sorption, the Darcy velocity, and the effective diffusion/dispersion coefficients. Both continuous and discrete adjoint approaches are considered. The partial differential equations associated with the adjoint system are derived based on the adjoint state theory for coupled problems. Physical interpretations of the adjoint states are given in analogy to results obtained in the theory of groundwater flow. For the homogeneous case, analytical solutions for primary and adjoint systems are derived and presented in closed forms. Numerically calculated solutions are compared to the analytical results and show excellent agreements. Insights from sensitivity analysis are discussed to get a better understanding of the values of sensitivity coefficients. The sensitivity coefficients are also computed numerically by finite differences. The numerical sensitivity coefficients successfully reproduce the analytically derived sensitivities based on adjoint states. A derivative-based global sensitivity method coupled with the adjoint state method is presented and applied to a real field case represented by a site currently being considered for underground nuclear storage in Northern Switzerland, "Zürich Nordost", to demonstrate the proposed method. The results show the advantage of the adjoint state method compared to other methods in term of computational effort.

1. Introduction

Sensitivity analysis of mathematical or numerical models describing physical processes is important for obtaining an enhanced understanding of system performance. It involves the computation of sensitivity coefficients. These coefficients reflect the sensitivities of user-defined scalar measures of system behavior or model performance, called performance measures, to various model parameters. For instance, they are used to determine the relative sensitivity of performance measures with respect to the parameters of the system (Lu & Vesselinov, 2015; Sykes et al., 1985; Wilson & Metcalfe, 1985), to guide gradient search in nonlinear optimization (Hayek et al., 2008), or to perform first- and second-order, second-moment uncertainty analyses (Li & Yeh, 1998).

Sensitivity coefficients are first derivatives indicating the rate of performance measure change caused by a small perturbation of the parameters. Literature review indicates that there are three methods, which are frequently used in the calculation of sensitivity coefficients: the influence coefficient method known also as the perturbation method (Yeh, 1986), the sensitivity method (Sun, 1994), and the adjoint state method (Chavent, 2009; Sun, 1994). The influence coefficient method uses the concept of parameter perturbation. It consists in perturbing each parameter (one at a time) by a small amount and solving the system of governing equations subject to the imposed initial and boundary conditions. The sensitivity coefficients are then obtained by finite differences. If there are N_p parameters to be investigated, then the system of governing equations has to be solved N_p+1 times to produce the sensitivity coefficients. The sensitivity method consists in deriving directly the performance measure with respect to the parameters. This involves the derivatives of the state variables (e.g., hydraulic head and concentrations) with respect to the parameters. Theses derivatives, known as the state sensitivities, are the solutions of the system of sensitivity equations. This latter is obtained by taking the partial derivatives with respect to each parameter in the governing equations and the initial and boundary conditions. The number of system of equations to be solved to generate the sensitivity coefficients is N_p

©2019. American Geophysical Union. All Rights Reserved.

+1, which is the same as that of the perturbation method. For problems with large number of parameters, the approaches based on the perturbation and sensitivity methods become prohibitively expensive. In this context, the adjoint sensitivity method is an alternative approach, which offers an elegant and computationally efficient way to compute the sensitivity coefficients. The adjoint methodology separates the sensitivity analysis into two distinct stages. The first one relates exclusively to the performance measure, while the second stage relates exclusively to the sensitivity parameter. The adjoint state from the first stage provides a link between the two stages. This method requires the resolution of an additional system called the adjoint state system. Therefore, for a given performance measure only two systems have to be solved (the primary system of governing equations and the adjoint state system) independently from the number of sensitivity parameters.

The adjoint state method has been used successfully in a wide range of disciplines such as mathematical physics, geophysics, systems engineering, economics, constrained optimization, nuclear engineering, electrical engineering, meteorology, oceanography, hydrogeology, petroleum engineering, and seismology. In hydrogeology, the adjoint state method has been employed in many applications including interpretation of interference tests using geostastistical techniques (de Marsily et al., 1984), steady-state groundwater flow (Sykes et al., 1985; Wilson & Metcalfe, 1985), groundwater travel time uncertainty analysis (LaVenue et al., 1989), automated calibration of transmissivity fields (LaVenue et al., 1995; RamaRao et al., 1995), coupled nonlinear multiphase multicomponent flow (RamaRao & Mishra, 1996), modeling multidimensional groundwater flow (Clemo, 2007), adaptive multiscale parameterization of flow in unsaturated porous media (Hayek et al., 2008), transient groundwater flow in a bounded model domain (Lu & Vesselinov, 2015), fractured dual-porosity media (Delay et al., 2017; Fahs et al., 2014), and coupled surface water-groundwater modeling (RamaRao et al., 2017). However, few applications of the adjoint state method have been devoted to solute transport (e.g., Larbkich et al., 2014; Michalak & Kitanidis, 2004; Neupauer & Wilson, 1999, 2001; Piasecki & Katopodes, 1997).

Motivated by the worldwide interest in geologic disposal of radioactive wastes, this work presents the adjoint state method applied to the problem describing sequentially coupled radionuclide (RN) transport in a steady-state regime. Indeed, geological waste repositories are constructed to isolate radioactive wastes from the environments in many countries. Performance assessments at potential nuclear waste repository sites require the capability to model coupled RN transport processes. The release of RNs from radioactive wastes through the geosystem is typically simulated using numerical models. The sensitivity of the numerical solution to model parameters is often of interest for the demonstration of safety of geologic disposal.

A full mathematical/numerical adjoint sensitivity model to calculate the sensitivity coefficients of transport parameters in heterogeneous porous media is presented. The model applies for an arbitrary number of RN decay chain members and the transport parameters include the RN retardation factors due to sorption, the Darcy velocity, and the effective diffusion/dispersion coefficients. Following the continuous adjoint state approach, the system of partial differential equations (PDEs) representing the adjoint states is derived according to the adjoint state theory for coupled problems (Sun, 1994). The sensitivity coefficients are then obtained by simple integration based on the analytical expressions. The discrete adjoint approach that consists in deriving the adjoint state equations of the numerical model directly from the discretized (matrix) equations associated with the primary problem is also presented. For the case of a homogeneous porous medium, analytical solutions to both primary and adjoint systems are derived for two performance measures: combination of RN concentrations at a point and combination of spatially integrated RN concentrations. Numerical solutions associated with primary and adjoint systems are implemented in MATLAB and compared to the analytical results. The analytical sensitivity coefficients are also compared to those obtained numerically using the perturbation method. Finally, a derivative-based global sensitivity method coupled with the adjoint state method is presented and applied to a real field case represented by a site currently being considered for underground nuclear storage in Northern Switzerland, "Zürich Nordost", to demonstrate the proposed method.

2. Mathematical Theory

2.1. Governing Equations

Sensitivity analysis of a model provides the first-order derivatives of some function J of the output variables with respect to the uncertain input parameters of the system. This function, which known as the

performance measure and also called the objective function, is a scalar measure of system behavior or model performance. In this work, we are interested in the model describing steady-state sequentially coupled RN transport in heterogeneous porous media. The governing equations for one-dimensional steady-state concentrations of N RNs undergoing advection, hydrodynamic dispersion, and sequential first-order decay reactions write for $i = 1,...,N$ and $0 \le x \le L$ as follows:

$$L_i \equiv \frac{\mathrm{d}}{\mathrm{d}x}\left(D_i \frac{\mathrm{d}C_i}{\mathrm{d}x}\right) - \frac{\mathrm{d}}{\mathrm{d}x}(VC_i) - \phi k_i R_i C_i + \phi k_{i-1} R_{i-1} C_{i-1} = 0 \tag{1}$$

where ϕ is the porosity of the porous medium (−), V is the Darcy velocity (ML^{-1}), and D_i, R_i, k_i, and C_i are the effective diffusion/dispersion coefficient (ML^{-2}), the retardation factor due to sorption (−), the decay constant (T^{-1}), and the concentration of the ith RN (ML^{-3}), respectively. In equation (1), L_i is the transport operator defining the ith transport equation. Note that $k_0 = 0$ indicating that L_1 involves only the parent RN concentration C_1. The parameters ϕ, V, D_i, and R_i are in general dependent on the space coordinate x. They are constant in the case of homogeneous porous medium.

Two problems are considered in this work. Problem A assumes prescribed concentrations (Dirichlet conditions) at the upstream boundary ($i = 1,...,N$):

$$L_{Bi} \equiv C_i(0) = C_i^0 \tag{2}$$

while prescribed fluxes (Neuman conditions) are considered for Problem B ($i = 1,...,N$)

$$L_{Bi} \equiv -V(0)C_i(0) + D_i(0)\frac{\mathrm{d}C_i}{\mathrm{d}x}(0) = -F_i^0 \tag{3}$$

where C_i^0 and $F_i^0 > 0$ are given prescribed concentration and flux associated with the ith RN at the upstream boundary. In equations (2) and (3), L_{Bi} is used to indicate the boundary operator of the ith transport equation.

For both problems, it is assumed that the RN concentrations are zero at the downstream boundary ($i = 1,...,N$):

$$C_i(L) = 0 \tag{4}$$

2.2. Sensitivity Coefficient

The general form of a performance measure associated with the above mathematical model may be written as an integral in the space domain as follows:

$$J = \int_0^L f(\mathbf{p}, \mathbf{C})\mathrm{d}x \tag{5}$$

where f is a function of the system state of the N-dimensional vector of concentrations $\mathbf{C} = (C_1, C_2, ..., C_N)^T$ and the vector $\mathbf{p} = \left(p_1, p_2, ..., p_{N_p}\right)^T$ of N_p system parameters. Any physical parameter (i.e., retardation factor of any RN, effective diffusion/dispersion coefficient associated with any RN, or Darcy velocity) could be a sensitivity parameter, p_k.

In equation (5), the function f is integrated over the length L of the spatial domain. This function could be any function of the concentrations vector. In sensitivity analysis, we are interested in computing the sensitivity of the performance measure with respect to a particular system parameter, p_k. One measure of this sensitivity is the first derivative of J with respect to p_k, denoted by $\partial J/\partial p_k$ and called herein the sensitivity coefficient. It can be evaluated by direct derivation of (5):

$$\frac{\partial J}{\partial p_k} = \int_0^L \left(\frac{\partial f}{\partial p_k} + \sum_{i=1}^{N} \frac{\partial f}{\partial C_i}\psi_{ik}\right)\mathrm{d}x \tag{6}$$

where $\psi_{ik} = \partial C_i/\partial p_k$ is the sensitivity of the RN concentration C_i with respect to the specified parameter p_k and is called the state sensitivity. For complicated problems finding the state sensitivities ψ_{ik} can be cumbersome and expensive. An alternative solution is the use of an adjoint approach, in which the sensitivity coefficients are given in terms of adjoint state functions $\lambda_i(x)$ associated with the state concentrations $C_i(x)$.

3. Adjoint Approach

Two alternative procedures are available for the derivation of the adjoint state equations associated with a numerical model: the continuous approach and the discrete approach. The continuous approach consists in deriving the partial differential equations of the adjoint state functions starting from those representing the primary problem (1) and then discretize them in the numerical model. The discrete approach consists in deriving the adjoint state equations directly from the discretized (matrix) equations associated with the primary problem (1). Both approaches are used in this work and they are presented below.

3.1. Continuous Approach

According to the theory of adjoint states for coupled problems (Sun, 1994), the vector of adjoint states $\boldsymbol{\lambda} = (\lambda_1, \lambda_2, ..., \lambda_N)^T$ is solution of the adjoint system defined by

$$\nabla^*_{\mathbf{C}} \mathbf{L} \boldsymbol{\lambda} + \frac{\partial f}{\partial \mathbf{C}} = \mathbf{0} \tag{7}$$

The associated boundary conditions are

$$\boldsymbol{\lambda} = \mathbf{0} \ \text{ or } \ \nabla^*_{\mathbf{C}} \mathbf{L}_{\mathbf{B}} \boldsymbol{\lambda} = \mathbf{0}, \ \text{ at } x = 0 \tag{8}$$

$$\boldsymbol{\lambda} = 0, \quad \text{at } x = L \tag{9}$$

The first equation of (8) (i.e., $\boldsymbol{\lambda} = \mathbf{0}$) is used when the primary problem is subject to Dirichlet boundary condition (Problem A), while the second equation (i.e., $\nabla^*_{\mathbf{C}} \mathbf{L}_{\mathbf{B}} \boldsymbol{\lambda} = \mathbf{0}$) is used when the primary problem is subject to Neumann boundary condition (Problem B).

The sensitivity coefficients are expressed in terms of the adjoint states as follows:

$$\frac{\partial J}{\partial p_k} = \int_0^L \left[\frac{\partial f}{\partial \mathbf{p}} + \nabla^*_{\mathbf{p}} \mathbf{L} \boldsymbol{\lambda} \right]_k \mathrm{d}x + \left[\nabla^*_{\mathbf{p}} \mathbf{L}_{\mathbf{B}} \boldsymbol{\lambda} \Big|_{x=0} \right]_k \tag{10}$$

In the above equations, $\nabla^*_{\mathbf{C}} \mathbf{L}$ and $\nabla^*_{\mathbf{p}} \mathbf{L}$ are the adjoint operators of matrices $\nabla_{\mathbf{C}} \mathbf{L}$ and $\nabla_{\mathbf{p}} \mathbf{L}$, gradient operators of $\mathbf{L} = (L_1, L_2, ..., L_N)^T$ with respect to $\mathbf{C}$ and $\mathbf{p}$, respectively. The definitions of operators $\nabla_{\mathbf{C}} \mathbf{L}$ and $\nabla_{\mathbf{p}} \mathbf{L}$ and their associated adjoint operators $\nabla^*_{\mathbf{C}} \mathbf{L}$ and $\nabla^*_{\mathbf{p}} \mathbf{L}$ are given in Appendix A.

In equation (10), $[\cdot]_k$ represents the kth component of $[\cdot]$. The first term $\int_0^L [\partial f / \partial \mathbf{p}]_k \mathrm{d}x$ represents the contribution of the performance measure. It can be calculated analytically by direct differentiation. This term vanishes when f is independent of the parameter in consideration. The second term $\int_0^L \left[\nabla^*_{\mathbf{p}} \mathbf{L} \boldsymbol{\lambda} \right]_k \mathrm{d}x$ involves the adjoint states solutions of the adjoint system (7)–(9). It can be calculated by simple integration after the evaluation of the elements of the adjoint matrix $\nabla^*_{\mathbf{p}} \mathbf{L}$. The last term $\left[\nabla^*_{\mathbf{p}} \mathbf{L}_{\mathbf{B}} \boldsymbol{\lambda} \Big|_{x=0} \right]_k$ indicates the effect of the boundary conditions. This term is an integral over the domain boundary. In the case of a one-dimensional problem, the boundary is restricted to the point ($x = 0$). This term vanishes when the boundary conditions are independent of the parameter in consideration. This holds for Problem A. However, this term has to be considered for the computation of the sensitivities $\partial J / \partial V$ and $\partial J / \partial D_i$ for Problem B where the boundary operators L_{Bi} depend on both V and D_i (see equation (3)). The transpose adjoint boundary operator $\nabla^*_{\mathbf{C}} \mathbf{L}_{\mathbf{B}}$ has the same form as $\nabla^*_{\mathbf{C}} \mathbf{L}$, except that $\mathbf{L}$ is changed to $\mathbf{L}_{\mathbf{B}} = (L_{B1}, L_{B2}, ..., L_{BN})^T$.

Using the definitions of the adjoint operators, the adjoint system (7) writes in form of PDEs as follows (see Appendix A for the detailed derivation):

$$\frac{\mathrm{d}}{\mathrm{d}x}\left(D_i\frac{\mathrm{d}\lambda_i}{\mathrm{d}x}\right)+\frac{\mathrm{d}}{\mathrm{d}x}(V\lambda_i)-\phi k_i R_i\lambda_i+\phi k_i R_i\lambda_{i+1}+\frac{\partial f}{\partial C_i}=0 \tag{11}$$

for $i = 1,...,N$ and $0 \le x \le L$.

In equation (11) $\lambda_{N+1} = 0$. This indicates that the Nth adjoint state is independent of those associated with the remaining RNs. Contrary to the transport system (1) where RN1 is the parent radionuclide (RN) and each RN concentration of the decay chain depends on its parent, the adjoint system has a backward behavior. The adjoint state variable λ_N associated with the RN N plays the role of parent of all state variables and so it is independent of all other λ_i.

The boundary conditions associated with equation (11) depend on the type of boundary conditions associated with the primary problem. They are given by

$$\lambda_i(0)=0,\quad \lambda_i(L)=0 \tag{12}$$

for Problem A, and

$$\frac{\mathrm{d}\lambda_i}{\mathrm{d}x}(0)=0,\quad \lambda_i(L)=0 \tag{13}$$

for Problem B.

A detailed discussion about the derivation of (12) and (13) is also provided in Appendix A.

Generally, the adjoint system of PDEs (11) together with boundary conditions (12) or (13) may be discretized and solved numerically by any numerical scheme to obtain the adjoint states. However, for specific cases (for some specific performance measures) the system may be solved analytically as shown later on.

The sensitivity coefficients may be obtained after using the solutions of systems (11) and (12) or (11) and (13) by applying (10). This latter may be rewritten as

$$\frac{\partial J}{\partial p_k}=\int_0^L\left[\frac{\partial f}{\partial p_k}+\sum_{i=1}^{N}\left[\frac{\partial L_i}{\partial p_k}\right]^*\lambda_i(x)\right]\mathrm{d}x+\sum_{i=1}^{N}\left[\frac{\partial L_{Bi}}{\partial p_k}\right]^*\lambda_i(0) \tag{14}$$

The terms $\partial f/\partial p_k$, $[\partial L_i/\partial p_k]^*$, and $[\partial L_{Bi}/\partial p_k]^*$ depend on the parameter of interest and on the solution of the primary problem, while the adjoint states λ_i depends only on the performance measure.

3.2. Discrete Approach

The discrete approach consists in deriving the adjoint state equations directly from the discretized equations associated with the primary problem. The discretized matrix system associated with problem (1) may be written in matrix form as follows:

$$[A_i]\{C_i^*\}+[B_i]\{C_{i-1}^*\}-\{G_i\}=\{0\} \tag{15}$$

where $\{C_i^*\}$ is the vector of unknown concentrations at nodes or elements of the discretized numerical grid and associated with the ith RN, $\{G_i\}$ is a known vector, which depends on the boundary conditions, and $[A_i]$ and $[B_i]$ are the matrices associated with the discretized numerical scheme. Note that $[B_1] = 0$ since the parent RN is independent of the other RNs. The system of matrix equation (15) can be solved successively by solving first the system associated with the parent RN (i.e., $[A_1]\{C_1^*\} = \{G_1\}$).

The discretized form of the performance measure (5) may be written as $J = F(\mathbf{p}, \mathbf{C}^*) = \sum_{k=1}^{n} f_k(\mathbf{p}, \mathbf{C}^*)$, where F and f_k are given scalar functions, which depend on the performance measure type and n is the number of nodes or elements.

Multiplying (15) by an arbitrary vector $\{\lambda_i^*\}$ of dimension n and summing for all $i = 1,...,N$, we get after adding the obtained summation to J

$$J = F(\mathbf{p}, \mathbf{C}^*) + \sum_{i=1}^{N} \{\lambda_i^*\}^T \left([A_i]\{C_i^*\} + [B_i]\{C_{i-1}^*\} - \{G_i\}\right) \tag{16}$$

The vector $\{\lambda_i^*\}$ is called the (discretized) adjoint state vector associated with the ith RN, which must be determined.

Deriving (16) with respect to a given sensitivity parameter p_k, we get

$$\frac{\partial J}{\partial p_k} = \frac{\partial F}{\partial p_k} + \sum_{i=1}^{N} \frac{\partial F}{\partial \{C_i^*\}} \frac{\partial \{C_i^*\}}{\partial p_k} + \sum_{i=1}^{N} \{\lambda_i^*\}^T \left(\frac{\partial [A_i]}{\partial p_k}\{C_i^*\} + \frac{\partial [B_i]}{\partial p_k}\{C_{i-1}^*\} - \frac{\partial \{G_i\}}{\partial p_k} + [A_i]\frac{\partial \{C_i^*\}}{\partial p_k} + [B_i]\frac{\partial \{C_{i-1}^*\}}{\partial p_k} \right) \tag{17}$$

After some mathematical manipulations, equation (17) can be rearranged to obtain

$$\frac{\partial J}{\partial p_k} = \frac{\partial F}{\partial p_k} + \sum_{i=1}^{N} \{\lambda_i^*\}^T \left(\frac{\partial [A_i]}{\partial p_k}\{C_i^*\} + \frac{\partial [B_i]}{\partial p_k}\{C_{i-1}^*\} - \frac{\partial \{G_i\}}{\partial p_k} \right) + \sum_{i=1}^{N} \left(\{\lambda_i^*\}^T [A_i] + \{\lambda_{i+1}^*\}^T [B_{i+1}] + \frac{\partial F}{\partial \{C_i^*\}} \right) \frac{\partial \{C_i^*\}}{\partial p_k} \tag{18}$$

In the derivation of equation (18) we assumed that $\{\lambda_{N+1}^*\} = \{0\}$. This is a necessary condition for the resolution of the adjoint system.

As the adjoint state vector $\{\lambda_i^*\}$ is arbitrary then terms in equation (18) containing $\frac{\partial \{C_i^*\}}{\partial p_k}$ can be eliminated by letting

$$\{\lambda_i^*\}^T [A_i] + \{\lambda_{i+1}^*\}^T [B_{i+1}] + \frac{\partial F}{\partial \{C_i^*\}} = \{0\} \tag{19}$$

Taking the transpose of (19), thus, the adjoint state system becomes

$$[A_i]^T \{\lambda_i^*\} + [B_{i+1}]^T \{\lambda_{i+1}^*\} + \frac{\partial F}{\partial \{C_i^*\}^T} = \{0\} \tag{20}$$

The discretized adjoint state system is solved first for $i = N$ by using the condition $\{\lambda_{N+1}^*\} = \{0\}$. Then, it can be solved successively and (forwardly) for $i = N-1, N-2, \ldots, 1$.

The sensitivity coefficient is then obtained from (18) as follows:

$$\frac{\partial J}{\partial p_k} = \frac{\partial F}{\partial p_k} + \sum_{i=1}^{N} \{\lambda_i^*\}^T \left(\frac{\partial [A_i]}{\partial p_k}\{C_i^*\} + \frac{\partial [B_i]}{\partial p_k}\{C_{i-1}^*\} - \frac{\partial \{G_i\}}{\partial p_k} \right) \tag{21}$$

Both continuous and discrete approaches give equivalent results. Sykes et al. (1985) intuitively believe the discrete approach to prove superior to the continuous one for the numerical simulation of the adjoint state functions. The discrete approach permits a simpler mathematical treatment, particularly in handling the boundary conditions. Moreover, the discrete approach uses the same matrix (or its transpose) of the linear system of the discretized primary problem. Therefore, the matrix is treated numerically once and for all, which allows a significant decrease of the computational costs. Samper and Neuman (1986) have shown that with respect to the advective-dispersive transport equations, both formulations (continuous and discrete) are consistent in that they converge to the same adjoint state partial differential equations as the spatial and temporal discretization intervals tend to zero. The continuous approach has the advantage that for specific forms of the performance measure, the adjoint system of PDEs (11) can be solved analytically. Therefore, analytical sensitivity coefficients could be derived and could be considered as reference solutions of numerical sensitivities.

3.3. Physical Interpretation of The Adjoint States

To provide an insight into the physical significance of the adjoint state functions, we assume that the transport operator L_i includes a source term denoted by Q_i defined by

$$Q_i(x) = Q_i^*\delta(x-x') \tag{22}$$

where Q_i^* is the strength of a source (associated with the ith RN) introduced in the field at a given point x'.

Therefore, equation (1) can be rewritten as follows:

$$L_i \equiv \frac{\mathrm{d}}{\mathrm{d}x}\left(D_i\frac{\mathrm{d}C_i}{\mathrm{d}x}\right) - \frac{\mathrm{d}}{\mathrm{d}x}(VC_i) - \phi k_i R_i C_i + \phi k_{i-1}R_{i-1}C_{i-1} + Q_i^*\delta(x-x') = 0 \tag{23}$$

Assume that we are looking for the sensitivity of the performance measure J with respect to Q_i^*. If the function f is explicitly independent of Q_i^* and if we take $\mathbf{p} = Q_i^*$ (i.e., Q_i^* is the sole parameter of interest), equation (10) reduces after applying the adjoint operators to

$$\frac{\mathrm{d}J}{\mathrm{d}Q_i^*} = \int_0^L \lambda_i(x)\delta(x-x')\mathrm{d}x = \lambda_i(x') \tag{24}$$

Equation (24) indicates that the adjoint state function $\lambda_i(x)$ associated with the ith RN is interpreted as the sensitivity coefficient for the parameter of steady source strength at x. It represents the rate at which the performance measure varies per unit source of RN Q_i^* ($MT^{-1}L^{-3}$) at x. The dimension of the adjoint states are those of the performance measure J times (TL^3/M), for the steady-state case considered here. This result is similar to previous results obtained in the theory of groundwater flow (Sykes et al., 1985; Wilson & Metcalfe, 1985).

4. Analytical Solutions

Exact analytical solutions for primary Problems A and B (i.e., equations (1)–(4)) are developed by applying the general method for solving multispecies coupled problems introduced by Clement (2001). These analytical solutions are presented in Appendix B. The details of derivation are given in supporting information Text S1.

Exact analytical solutions for the adjoint problems (11)–(13) are also derived by applying the same method. These solutions are associated with two kinds of performance measure. The first one is defined as a combination of RN concentrations at a given point x_0 ($0 < x_0 < L$):

$$J = \sum_{i=1}^{N}\alpha_i C_i(x_0) = \sum_{i=1}^{N}\alpha_i\int_0^L\delta(x-x_0)C_i(x)\mathrm{d}x \tag{25}$$

The second one is defined as a combination of spatially integrated RN concentrations as follows:

$$J = \sum_{i=1}^{N}\beta_i\int_0^L C_i(x)\mathrm{d}x \tag{26}$$

where α_i and β_i are some positive coefficients.

The performance measure (25) can be used to represent the total/partial concentration at a point, while that defined by (26) can be used to represent the total mass or the mass of a specific RN remaining in the system at steady state.

The function f associated with the performance measures (25) and (26) and appearing in equations (5) and (11) can be written as $f(x) = \sum_{i=1}^{N}\alpha_i\delta(x-x_0)C_i(x)$ and $f(x) = \sum_{i=1}^{N}\beta_i C_i(x)$, respectively.

The exact solutions associated with (25) and (26) are presented in Appendix C. The details of derivation are provided in supporting information Text S2.

Table 1
Porous Medium and RN Parameter Values Used in the Applications

Parameter	Value
L (m)	100
ϕ (−)	0.3
V (m/year)	10^{-4}
D (m^2/year)	2×10^{-2}
R_1 (−)	3
R_2 (−)	4
R_3 (−)	1
k_1 ($year^{-1}$)	3×10^{-4}
k_2 ($year^{-1}$)	2×10^{-4}
k_3 ($year^{-1}$)	4.5×10^{-4}
C_1^0 (mol/m^3)	100
C_2^0 (mol/m^3)	50
C_3^0 (mol/m^3)	10
F_1^0 (mol·m^{-3}·$year^{-1}$)	1
F_2^0 (mol·m^{-3}·$year^{-1}$)	0.1
F_3^0 (mol·m^{-3}·$year^{-1}$)	0

Analytical expressions of sensitivity coefficients with respect to retardation factors, Darcy velocity, and effective diffusion/dispersion coefficients are also provided in supporting information Text S3.

5. Numerical Experiments

The numerical experiments shown below are divided into two parts. The first part aims to validate the developed analytical adjoint state model using the continuous approach and to provide some insights from sensitivity analysis based on the obtained results. In the second part, a derivative-based global sensitivity method coupled with the adjoint state method is used for identifying important/unimportant parameters associated with a real field case represented by a site (Zürich Nordost) currently being considered for underground nuclear storage in Northern Switzerland.

5.1. Validation of Analytical Adjoint Equations

To illustrate the theory presented in this work, we consider an example of three-member decay chain where Radionuclide 1 (RN_1) decays into Radionuclide 3 (RN_3) in a homogeneous porous medium of length L according to the sequential decay chain $RN_1 \rightarrow RN_2 \rightarrow RN_3$. In this chain, RN_1 is the parent RN, RN_2 is the daughter, and RN_3 is the granddaughter. The porous medium and RN properties are presented in Table 1. These data are synthetic but are in the range of real values.

To insure the correctness of the analytical solutions of the primary problems, they are compared with numerical solutions. The system of equations (1) together with boundary conditions (2)–(4) are implemented in MATLAB using the numerical solver "pdepe" (www.mathworks.com). This solver solves initial-boundary value problems for systems of parabolic and elliptic PDEs in the one space variable and time. Here, the numerical solutions were run until reaching convergence to the steady-state solutions. A small and constant mesh size $\Delta x = 0.01$ m is used in the numerical examples to avoid numerical dispersion. Figure 1 shows the concentrations profiles obtained from the analytical (solid lines) and numerical (symbols) solutions from Problem A (a) and Problem B (b), respectively. The values of the boundary concentrations and boundary fluxes used in these examples are presented in Table 1. The figures show excellent agreements between the numerical and analytical solutions for all RN concentrations and for both problems.

5.1.1. Adjoint State Variables

This section explores some features of the adjoint state variables associated with the performance measures defined by (25) and (26).

5.1.1.1. Total RN Concentration

The first performance measure represents the value of the total concentration at the domain center $x_0 = L/2$. By total concentration, we mean the sum of all RN concentrations. Therefore, $X_0 = x_0/L = 0.5$ and all α_i are equal to 1 in equation (25). The adjoint state variables associated with the total concentration at $X_0 = 0.5$ are depicted in Figure 2. The analytical adjoint states are also compared with numerical solutions obtained by solving the adjoint system (11) with boundary conditions (12) or (13) using the MATLAB pdepe solver. The figures show excellent agreements between numerical and analytical results. Figure 2a (resp. Figure 2b) shows that for Problem A (resp. Problem B), each adjoint state has a maximum peak at $X_0 = 0.5$ and then decreases toward the boundaries. The adjoint state profiles exhibit discontinuities of the derivatives at the peaks since they are also Green's functions. As discussed in section 3.3, the adjoint states $\lambda_i(X)$ represent the change in the total concentration at X_0 for a unit source of the ith RN at $X = x/L$. For Problem A, a unit source of RN at the left and right boundaries will immediately leave the system and has no impact on the total concentration since, by definition, the adjoint states vanish at the boundaries (see equation (12)). For each RN, the greatest impact on the total concentration at X_0 (i.e., the largest adjoint state value) occurs when the unit source is positioned at X_0. This is expected because for each RN the adjoint state is composed of two parts: an increasing part in the region $0 \leq X \leq X_0$ and a decreasing part in the region $X_0 \leq X \leq 1$. For Problem B, the same conclusion can be obtained with the exception that a unit source of RN at the left boundary may have an impact on the total concentration since the condition at this

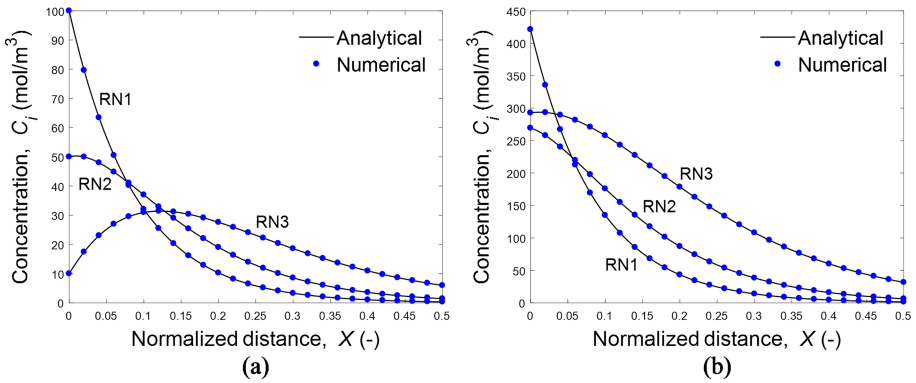

Figure 1. Analytical and numerical solutions for radionuclide (RN) concentrations corresponding to Problem A (a) and Problem B (b).

boundary is $d\lambda_i/dx = 0$ (see equation (13)) and so in general $\lambda_i(0) \neq 0$. However, the greatest impact on the total concentration at X_0 will always occur when the unit source is positioned at X_0 because the adjoint state value at the left boundary will never exceed $\lambda_i(X_0)$ (i.e., $\lambda_i(0) \leq \lambda_i(X_0)$). This conclusion can be drawn from the inspection of equation (C4), which shows that $\widetilde{\lambda}_i(X)$ is an increasing function from 0 to X_0 and so is $\lambda_i(X)$ (see equation (C2)).

Note that for both problems, at any position X in the domain, the change in the total concentration at X_0 is mostly affected by a unit source associated with the parent radionuclide RN_1, while the granddaughter radionuclide RN_3 has the smallest impact among all RNs (i.e., $\lambda_1(X) \geq \lambda_2(X) \geq \lambda_3(X)$).

5.1.1.2. Total RN Mass

The second performance measure represents the value of the total RN mass remaining in the system so that $\beta_i = \phi R_i$ in equation (26) for $i = 1,2,3$. The analytical and numerical solutions corresponding to Problems A and B are shown graphically in Figures 3a and 3b, respectively. Again, excellent agreements between both solution types are obtained for all RNs. Contrary to the previous case (of total concentration where the adjoint states are Green's functions representing discontinuities of the derivatives at the observation point), here the adjoint states are smooth functions of the space variable. For Problem A, the adjoint states have parabolic shapes, and each one reaches its maximum at some position between $X = 0$ and $X = 1$. The position of the maximum is not necessary the same for all RNs. It depends on the porous medium and RN properties. For the set of parameter values used here, all adjoint state functions have their maximums at

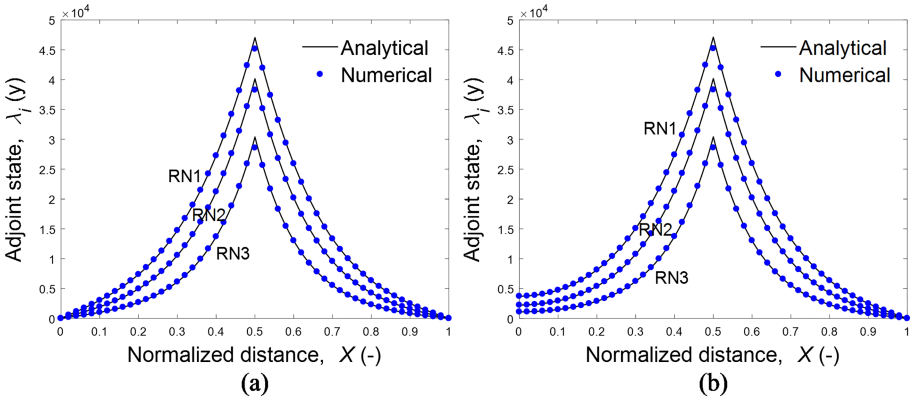

Figure 2. Analytical and numerical adjoint states corresponding to Problem A (a) and Problem B (b) and associated with the performance measure defined by (25). RN = radionuclide.

approximatively the middle of the domain. Therefore, for the current set of parameter values, a unit source at the center of the system has the greatest impact on the total mass. However, different parameter values would give different results. For instance, increasing the Peclet number P_e (=LV/D) to 50 (i.e., the current P_e equals to 0.5) would shift the maximums to the left. For Problem B, the adjoint state are decreasing functions of X as shown in Figure 3b. This characteristic of the adjoint state functions is independent from the parameter values. Indeed, a simple inspection of equation (C8) shows that

$$\frac{d\widetilde{\lambda}_i}{dX}(X) = -\frac{2L^2}{D}\left[\beta_i + \sum_{j=i+1}^{N}\left(\prod_{l=i}^{j-1}\frac{K_l}{K_{l+1}-K_i}\right)\beta_j\right]\frac{e^{\frac{P_e}{2}(1-X)}\varphi_i(X)}{P_e\Phi_i(0)+\sqrt{P_e^2+4K_i}\Psi_i(0)} \leq 0 \tag{27}$$

Therefore, $\widetilde{\lambda}_i(X)$ is a decreasing function of X and so is $\lambda_i(X)$ (see equation (C1)).

In addition, we have by definition $d\lambda_i/dx = 0$ (see equation (13)). Therefore, the maximum is reached at the left boundary and, as a conclusion, a unit RN source at this boundary ($X = 0$) has the greatest impact on the total mass in the system.

It should be mentioned that the shapes of the adjoint state functions shown in Figures 2 and 3 are independent from the "values" of the prescribed boundary conditions. They only depend on the boundary condition "type" (prescribed concentrations or fluxes). This can be easily seen from the mathematical expressions (C2)–(C5), and (C6) and (C7), which are independent of C_i^0 and F_i^0.

5.1.2. Sensitivities

Sensitivity coefficients of the various parameters can be analytically calculated with the help of adjoint states using the mathematical expressions presented in supporting information Text S3. The performance measure representing the total RN mass in the system is used. For the example of three-member decay chain, five parameters are considered that are R_1, R_2, R_3, V, and D.

The analytical sensitivity coefficients corresponding to Problems A and B are presented in Table 2. Negative values indicate that a parameter increase (resp. decrease) will result in a decrease (resp. increase) of the performance measure. The values indicate that for Problem A, Darcy velocity is the most sensitive parameter, followed by the effective diffusion/dispersion coefficient, and then by the retardation factors of the parent, daughter and granddaughter RNs, respectively. All these parameters are positive indicating that an increase in one of these parameters will increase the total mass of RNs in the system. For Problem B, again, Darcy velocity gives the highest sensitivity value (in absolute value), followed by the effective diffusion/dispersion coefficient. However, the retardation factor of the granddaughter RN is the most sensitive parameter among those of the three RNs contrary to Problem A. Moreover, the sensitivity coefficients of V and D are negative while those of the retardation factors are positives. Therefore, Darcy velocity and effective diffusion/dispersion coefficients have an opposite effect on the total mass.

5.1.2.1. Insights From Sensitivity Analysis

To have a better understanding of the values presented in Table 2, we recall the definition of the sensitivity coefficient $\partial J/\partial p_k$, which represents the change in the performance measure to the change in the parameter. It can be loosely thought of as the change in the value of J for a unit increase in the value of p_k and it is referred to as the "marginal sensitivity coefficient" (Sykes et al., 1985). For the current set of parameter values, a unit increase of the retardation factors of the parent RN R_1 (from 3 to 4), the daughter RN R_2 (from 4 to 5), and the granddaughter RN R_3 (from 1 to 2) represents 33.3333%, 25%, and 100% increase in the initial value of each parameter, while a unit increase in the value of the Darcy velocity V (from 0.0001 to 1.0001 m/year) and the value of the effective diffusion/dispersion coefficient D (from 0.02 to 1.02 m^2/year) represents 1,000,000% and 5,000% increase in their initial values. This explains the large values of their associated sensitivity coefficients. Therefore, the marginal sensitivity coefficients are local derivatives and are related to the assumed initial parameter value. The value of the sensitivity coefficient will generally be small for small changes and large for large changes in the initial value.

In sensitivity analysis, the performance of a system is often investigated in term of the normalized sensitivity coefficient S_{p_k}, which is defined as the value of the marginal sensitivity coefficient weighted by the initial value of the parameter to the value of the performance measure:

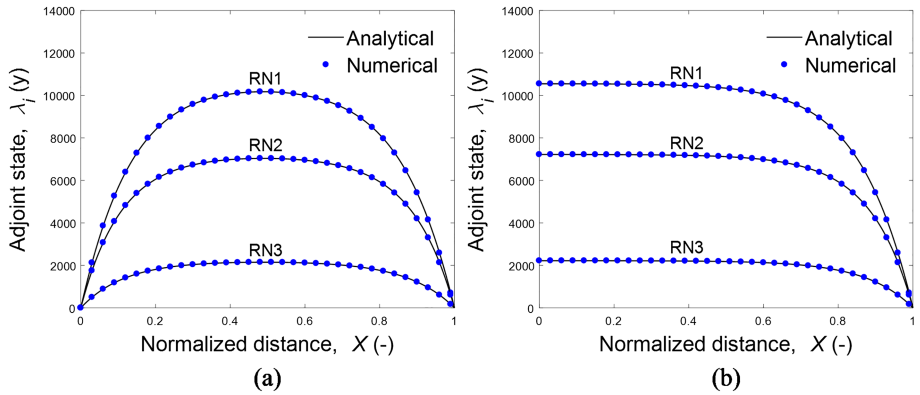

Figure 3. Analytical and numerical adjoint states corresponding to Problem A (a) and Problem B (b) and associated with the performance measure defined by (26). RN = radionuclide.

$$S_{p_k} = \frac{p_k}{J}\frac{\partial J}{\partial p_k} = \frac{\partial(\ln J)}{\partial(\ln p_k)} \tag{28}$$

The normalized sensitivity coefficient can be thought of as the percent change in the performance measure J caused by a 1% change in the value of the parameter. It represents a common basis for comparing the effect of system parameters to the performance measure.

Table 3 shows the analytically calculated normalized sensitivity coefficients corresponding to Problems A and B. The analytical expressions of the performance measure associated with Problems A and B are provided in supporting information Text S4. The table shows that, in contrast to the results obtained for the marginal sensitivity coefficients, the Darcy velocity is the less sensitive parameter among all other parameters, while the effective diffusion/dispersion coefficient is the most sensitive for both Problems A and B. However, the sensitivity coefficients of the retardation factors maintain their hierarchy of parameter importance.

The total of cumulative variation dJ of the performance measure is given for a system of N_p parameters as follows:

$$\mathrm{d}J = \sum_{k=1}^{N_p} \frac{\partial J}{\partial p_k}\mathrm{d}p_k \tag{29}$$

It represents the net change in the performance measure J and defined as the sum of all marginal sensitivities weighted by the variation of each parameter dp_k.

As discussed above, it is often preferred to work with the normalized sensitivities. Therefore, the normalized total sensitivity is defined as sum of all marginal sensitivities as follows:

Table 2
Analytical (Adjoint State Method) and Numerical (Perturbation Method) Sensitivity Coefficients $\partial J/\partial p_k$ Associated With Problems A and B for the Performance Measure Representing the Total RN Mass

	Sensitivity coefficient $\partial J/\partial p_k$			
	Problem A		Problem B	
Parameter (p_k)	Analytical	Numerical	Analytical	Numerical
R_1	182.7394	182.7378	2.4643	2.4542
R_2	116.9546	116.9530	2.2564	2.2482
R_3	86.0131	86.0091	15.0666	15.0405
V	7.3818×10^5	7.3830×10^5	-1.6185×10^4	-1.6158×10^4
D	5.4468×10^4	5.4468×10^4	-1.4933×10^3	-1.4892×10^3

Table 3
Analytically Calculated Normalized Sensitivity Coefficients $\partial J(lnJ)/\partial(lnp_k)$ Obtained by the Adjoint State Method for the Performance Measure Representing the Total RN Mass

	Normalized sensitivity coefficients $\partial J(\ln J)/\partial(\ln p_k)$	
Parameter (p_k)	Problem A	Problem B
R_1	0.2420	6.5596×10^{-4}
R_2	0.2065	8.0083×10^{-4}
R_3	0.0380	0.0013
V	0.0326	-1.4361×10^{-4}
D	0.4809	−0.0027

$$S_{\text{tot}} = \frac{\mathrm{d}(\ln J)}{\mathrm{d}(\ln \mathbf{p})} = \sum_{k=1}^{N_p} \frac{p_k}{J}\frac{\partial J}{\partial p_k} = \sum_{k=1}^{N_p} S_{p_k} \tag{30}$$

In our example we have

$$S_{\text{tot}} = S_{R_1} + S_{R_2} + S_{R_3} + S_V + S_D \tag{31}$$

It can be seen from Table 3 that for Problem A, a 1% increase in each of the five parameters gives $S_{\text{tot}} = 1$, while for Problem B a 1% increase in each parameter results in $S_{\text{tot}} \approx 0$.

5.1.2.2. Inspectional Analysis

Numerical sensitivity coefficients are also computed to compare with the analytical sensitivity coefficients based on adjoint states. The perturbation method is used to compute the numerical sensitivity coefficients based on the numerical solutions of the primary problems. Each sensitivity coefficient is calculated using the following formula:

$$\frac{\partial J}{\partial p_k} \approx \frac{J_n(p_k + \delta_k) - J_n}{\delta_k} \tag{32}$$

where δ_k is a parameter dependent small perturbation coefficient and J_n is the performance measure calculated from equation (26) based on the numerically calculated concentrations. The integrals are computed using the trapezoid rule. The perturbation coefficient δ_k is calculated as $(p_k/100) \times 10^{-6}$ so it represents 10^{-6}% change of the initial parameter value. The evaluation of (32) requires an additional numerical run of the primary problem for each parameter. Thus, in total, six numerical runs are required for each problem (1 for calculating J_n and 1 for each perturbed parameter).

Table 2 shows also the numerically calculated sensitivity coefficients for both problems. The values compare well with the analytical sensitivity coefficients presented in the same table. The slight differences between the values are due to the space discretization of the numerical solutions.

We would like to mention that the results presented here are not general and they are strictly dependent on the reference values and properties of both porous medium and RNs. Figure 4 shows for Problems A and B the variation of the normalized sensitivity coefficient with respect to a single parameter when the other parameters are kept to their initial values. The curves associated with Darcy velocity (upper figures) and effective diffusion/dispersion coefficient (middle figures) are bell shaped for Problem A and decreasing functions for Problem B. The curves associated with the retardation factors (bottom figures) are increasing functions for both problems. However, they stabilize at large values for Problem A, while they keep increasing for Problem B. These results show how the parameters "importance" depend on their reference values. For instance, for Problem A, if the reference Darcy velocity is 3×10^{-3} instead of 10^{-4} m/year, its normalized sensitivity coefficient jumps from 0.0326 to 0.626 and becomes the most sensitive parameter. Similarly, if the reference effective diffusion/dispersion coefficient is 2×10^{-5} instead of 2×10^{-2} m^2/year, then its normalized diffusion coefficient falls to 0.1402. This is expected because for such values ($V = 3 \times 10^{-3}$ m/year and $D = 2 \times 10^{-5}$ m^2/year) the transport is mainly advective ($P_e = 15{,}000$) and so the total mass is mainly affected by the change in the value of Darcy velocity. The figures associated with the retardation factors (bottom figures) show that the retardation factors are the most important parameters if their reference values are of the order of 10^3–10^4 (highly sorbing RNs).

The analytical sensitivity coefficients are useful also to identify "important regions" in the parameters space. By important regions we mean regions (showing combined effect of two or more parameters) in which the parameters values have large effects (large sensitivities) on the performance measure. For example, if the values of the retardation factors are kept at their initial reference values presented in Table 1, the important regions of the (V,D) space can be identified by using the 2-D plot showing the combined total sensitivity $S_V + S_D$ as function of the couple (V,D). Figure 5 shows that the important region is located in the region $8 \times 10^{-4} \le V \le 8 \times 10^{-3}$, $10^{-3} \le D \le 2 \times 10^{-2}$. Therefore, any value of (V,D) in this region results in a considerable effect on the value of the performance measure.

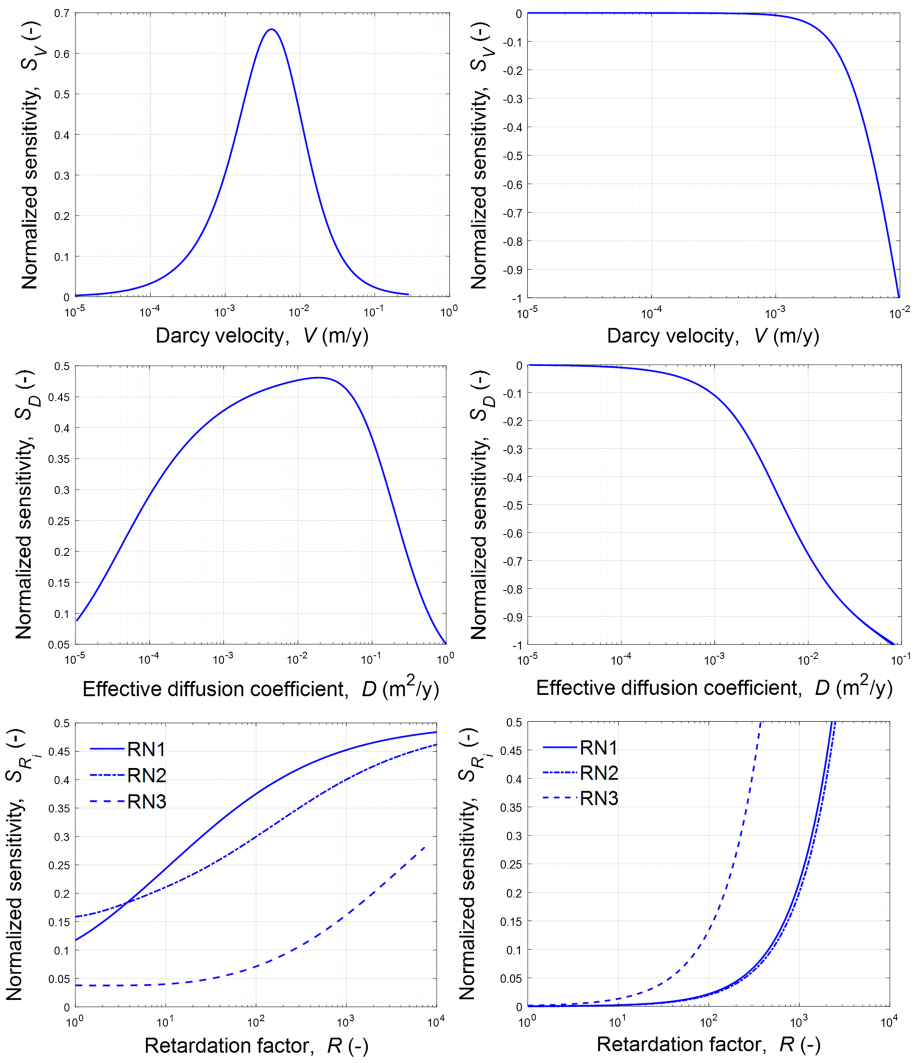

Figure 4. Normalized sensitivity coefficients for Darcy velocity (top figures), effective diffusion/dispersion coefficient (middle figures), and retardation factors (bottom figures) associated with Problem A (left column) and Problem B (right column). RN = radionuclide.

Finally, it is important to mention that different decay chains of RNs would in general give different results even when the porous medium properties are the same. As a conclusion, a global sensitivity method becomes necessary to correctly identify the important parameters of the model.

5.2. Derivative-Based Global Sensitivity Method Coupled With Adjoint Method

It has been shown previously that the local sensitivity coefficients $\partial J(\mathbf{p}^*)/\partial p_k$ depends on the nominal point $\mathbf{p}^*$ and it changes with a change of $\mathbf{p}^*$. This deficiency can be overcome by averaging $\partial J(\mathbf{p})/\partial p_k$ for a randomly selected set of parameter vector $\mathbf{p}$.

Kucherenko et al. (2009) presented a derivative-based global sensitivity measures (DGSM) method which is based on averaging local derivatives using Monte Carlo or quasi Monte Carlo sampling methods. These measures (or indices) are defined for each parameter p_k as follows:

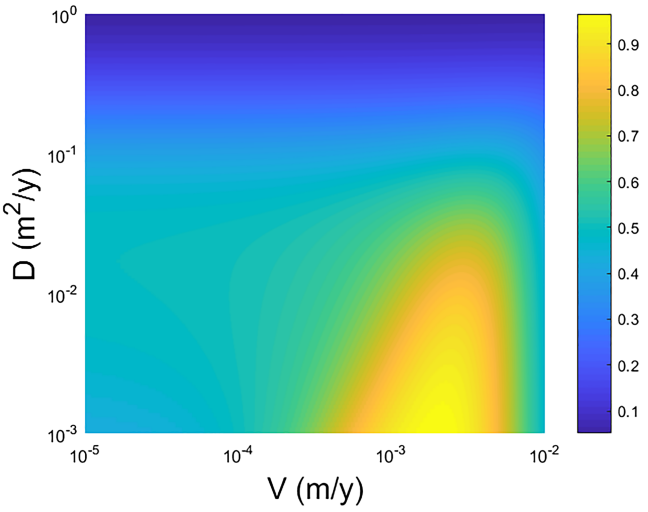

Figure 5. The 2-D plot of the variation of the combined total sensitivity S_V+S_D as function of (V,D).

$$M_k = \int_{H^{N_p}} \left|\frac{\partial J}{\partial p_k}\right| \mathrm{d}p_k \tag{33}$$

and

$$\sum_k = \left[\int_{H^{N_p}} \left(\left|\frac{\partial J}{\partial p_k}\right| - M_k\right)^2 \mathrm{d}p_k\right]^{1/2} \tag{34}$$

where H^{N_p} is the unit hypercube ($0 \le p_k \le 1$, $i = 1,...,N_p$).

The measure M_k is equivalent to the mean μ_k, while Σ_k is equivalent to the standard deviation σ_k. These measures could be used for identifying important/unimportant parameters by using the scatter plot M_k versus Σ_k.

The calculation of DGSM indices is based on the evaluation of integrals, which is easily performed using classical Monte Carlo, quasi Monte Carlo or Latin Hypercube Sampling. The empirical estimator of a given integral $\int_{H^{N_p}} f(\mathbf{x})\mathrm{d}\mathbf{x}$ is

$$I[f] = \frac{1}{R}\sum_{i=1}^{R} f(\mathbf{x}_i) \tag{35}$$

where $\{\mathbf{x}_i\}$ is a sequence of random points in H^{N_p} of length r (r is the number of random realization).

Kucherenko et al. (2009) compared the DGSM with Morris (1991) and Sobol (1993) sensitivity indices methods and shown that there is a link between DGSM and Sobol sensitivity indices. They have shown also that the computational time required for the numerical evaluation of DGSM is lower than that for the Morris method and many orders of magnitude lower than that for estimation of Sobol's sensitivity indices.

In this section, we use the DGSM method coupled with the adjoint state method for computing sensitivity coefficients in order to identify important/unimportant parameters of a numerical model. We consider the model representing the geological siting area Zürich Nordost north east of the city of Zürich in Switzerland. This siting area was proposed by NAGRA (National Cooperative for the Disposal of Radioactive Waste) as a potential geological siting region for a high-level waste repository for further investigation in Stage 3 of the Sectoral Plan for Deep Geological Repositories (SFOE, 2008). Figure 6 (left) shows the schematic stratigraphic-hydrogeological profile for this siting area. Several scenarios for modeling RN release from the barrier system have been adopted (see Nagra, 2014). The reference scenario is applied here, which consists in modeling the real geological formation as a layered system composed of six layers that are (see Figure 6, right): the Opalinus clay host rock (OPA) where the waste is embedded, the lower confining units represented by the formation Toniger Lias (TL), and the upper confining units represented by the Dogger formations (Sandkalkabfolgen (BD-SKA), Tonige Abfolgen and Sandig-tonige Abfolgen (BD-TA-STA)) and the Effingen beds (Kalkbankabfolgen (EFF-KBA) and Kalkmergelabfolgen (EFF-KMA)), respectively.

We consider a system containing a single RN that is Uranium-235 (^{235}U). Uranium-235 is assumed to be released at the center of the host rock (OPA) at a constant rate $Q = 2 \times 10^{-6}$ m^3/year. Zero concentration boundary conditions are imposed at the top and bottom boundaries of the layered system, which are considered as the interfaces between geosphere and biosphere (see Figure 6, right). It is assumed that the transport is mainly dominated by diffusion (because of the low permeability of OPA) so that $V = 0$. Equation (1) at which we add a source term (representing the release of ^{235}U) is discretized numerically for $i = 1$ using a centered finite volume scheme. The discretized equations can be written in matrix form (15) with $i = 1$. All layer parameters are assumed to be at their reference values (which are taken from Nagra, 2014, and presented in Table 4) except for the effective diffusion coefficients and the sorption coefficients, which are subject to uncertainties. They can have values between a lower value and an upper value. Lower and upper values for each layer parameters are also presented in Table 4 (taken from Nagra, 2014). The model contains then 12 uncertain parameters p_k ($k = 1,...,12$) with p_k ($k = 1,...,6$) represent the effective diffusion coefficients of

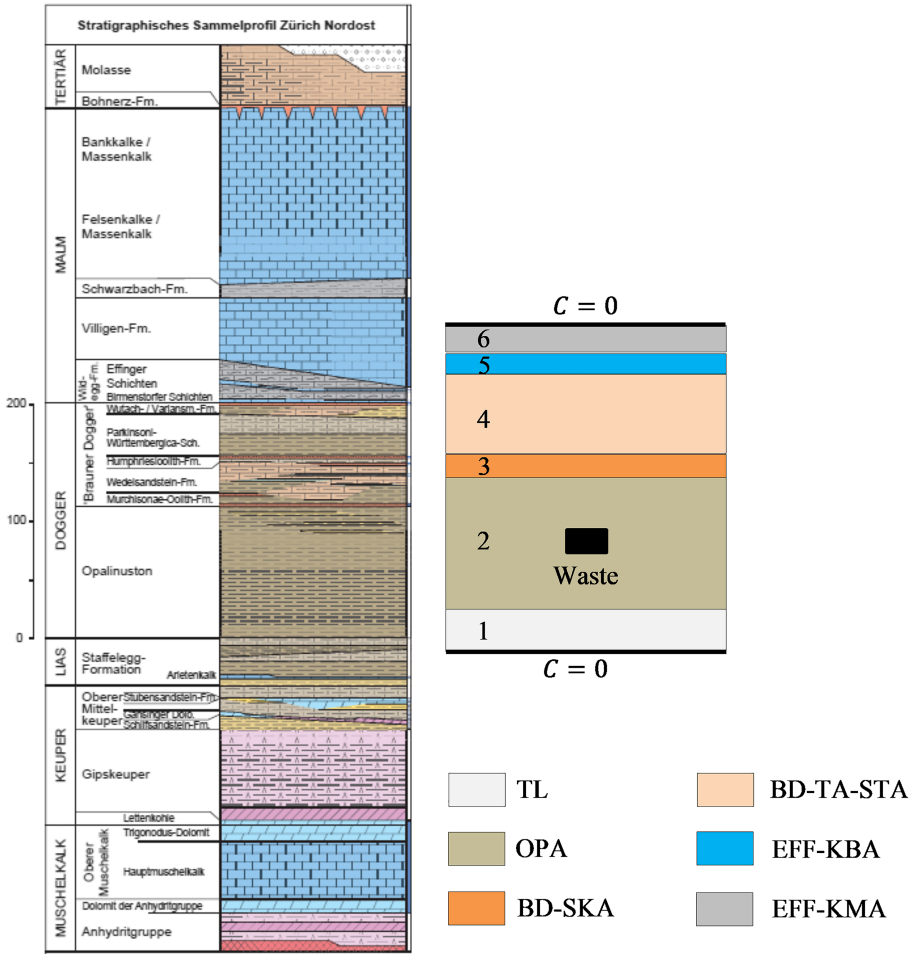

Figure 6. (left) Schematic stratigraphic-hydrogeological profile for the siting area Zürich Nordost (reproduced with permission of Nagra, NTB 14-03, Nagra, 2014, Figures A4–3). (right) Modeling concept for radionuclide transport.

layers TL, OPA, BD-SKA, BD-TA-STA, EFF-KBA, and EFF-KMA, respectively; and p_{k+6} ($k = 1,...,6$) represent the retardation factors of layers TL, OPA, BD-SKA, BD-TA-STA, EFF-KBA, and EFF-KMA, respectively. Note that the retardation factor is obtained from the value of the sorption coefficient (or distribution coefficient) K_d using the formula $R = 1+\rho K_d/\phi$, where ρ is the layer (rock) density and ϕ is the layer porosity.

Table 4
Parameter Values Used for the Example Presented in Section 5.2

		Parameters								
					D (m^2/s) (p_k)			K_d (m^3/kg) (p_{k+6})		
k	Layer	L (m)	ϕ (−)	ρ (kg/m^3)	RV	LV	UV	RV	LV	UV
1	TL	32	0.1	2,500	4×10^{-12}	2.6×10^{-13}	1.7×10^{-11}	0.2	0.01	0.6
2	OPA	110	0.11	2,410	5×10^{-12}	5×10^{-13}	2×10^{-11}	0.2	0.008	0.2
3	BD-SKA	10	0.1	2,440	4×10^{-12}	4×10^{-13}	2×10^{-11}	0.04	0.001	0.04
4	BD-TA-STA	80	0.12	2,440	6×10^{-12}	4×10^{-13}	2×10^{-11}	0.2	0.004	0.2
5	EFF-KBA	4	0.045	2,610	9×10^{-13}	2×10^{-13}	8×10^{-12}	3	0.01	3
6	EFF-KMA	11	0.09	2,500	3×10^{-12}	5×10^{-13}	1×10^{-11}	6	0.05	6

Note. LV = lower value; RV = reference value; UV = upper value.

Table 5
Sensitivity Coefficients Obtained by the Adjoint State Method (Discontinuous Approach) and the Perturbation Method for the Example Presented in Section 5.2 Using the Reference Values of All Parameters

		Sensitivity coefficient			
		Effective diffusion coefficient (p_k)		Retardation factor (p_{k+6})	
k	Layer	Adjoint state method	Perturbation method	Adjoint state method	Perturbation method
1	TL	9.7172×10^{-5}	9.7172×10^{-5}	-1.4258×10^{-12}	-1.4258×10^{-12}
2	OPA	8.3550×10^{-5}	8.3550×10^{-5}	-3.6619×10^{-12}	-3.6619×10^{-12}
3	BD-SKA	-1.7368×10^{-8}	-1.7368×10^{-8}	-1.0043×10^{-15}	-1.0042×10^{-15}
4	BD-TA-STA	3.9337×10^{-8}	3.9337×10^{-8}	-2.3507×10^{-15}	-2.3506×10^{-15}
5	EFF-KBA	1.2499×10^{-7}	1.2499×10^{-7}	-3.0738×10^{-17}	-3.0738×10^{-17}
6	EFF-KMA	9.7046×10^{-8}	9.7047×10^{-8}	-5.5046×10^{-17}	-5.5041×10^{-17}

The performance measure of interest is the total diffusive flux leaving the system at the interfaces geosphere/biosphere (i.e., the sum of RN fluxes at the top and bottom). For any given uncertain parameter, the sensitivity of the performance measure can be obtained by applying the discrete approach presented in section 3.2 . The adjoint states are then solutions of the linear adjoint system (20). The sensitivity coefficient of a parameter p_k at a given initial guess of parameters is obtained using equation (21). To validate the discrete approach, we first assume that effective diffusion coefficients and sorption coefficients are at their reference values. The results are then compared with other numerical results obtained from the perturbation method. Table 5 shows excellent agreement between both methods.

We are interested in identifying important/unimportant parameters, or in other words, we aim to answer the question: to which parameters the RN flux leaving the system is most sensitive?

To do so, we use the DGSM method coupled with the adjoint state method. We consider a sequence of quasi-random points $\{\mathbf{p}_i\}$ of length r, where $\mathbf{p}_i = (p_{1,i}, p_{2,i}, ..., p_{12,i})$, $i = 1,...,r$. The quasi-random points correspond to the so-called Sobol sequence (Sobol, 1976, 1998). This technique is based on the generation of deterministic quasi-random sequences with a good space-filling property of the parameter space. Thus, the parameter space is well covered for fairly small sets. In addition, the points of the Sobol sequence are independent so that by enriching the design sequentially, we keep the space-filling properties of the Sobol sequence.

For each realization $i = 1,...,r$, the primary and adjoint system are solved once. Thus, the total number of required calculations is $2r$. Figure 7 shows the scatter plots M_k versus Σ_k for $r = 100$ (a) and $r = 1{,}000$ (b), respectively. The numbers k inside the plots correspond to the parameter p_k. The parameters that have high M_k and high Σ_k are important, while the parameters that have low M_k and Σ_k are relatively unimportant. It can be observed that both sequences of realizations ($r = 100$ and $r = 1{,}000$) give similar results. The important parameters are p_2 (the effective diffusion coefficient of the host rock OPA), p_1 (the effective diffusion

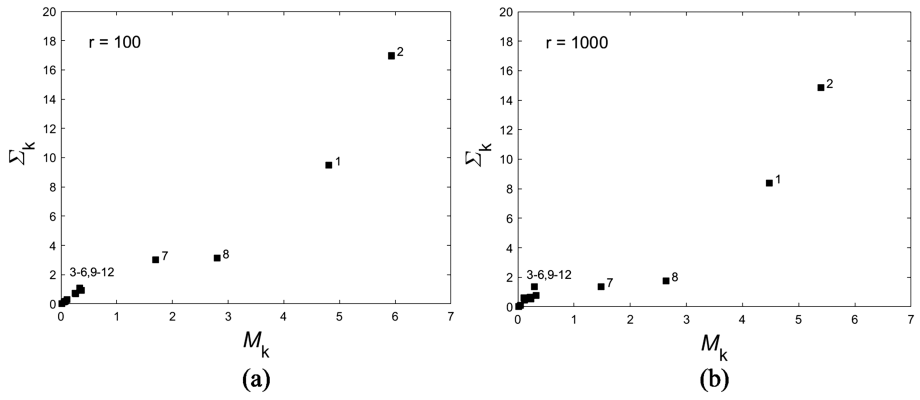

Figure 7. Estimated derivative-based sensitivity measures M_k and Σ_k for the cases: (a) $r = 100$ and (b) $r = 1{,}000$, associated with the example presented in section 5.2.

coefficient of the TL), p_8 (the retardation factor of the host rock OPA), and p_7 (the retardation factor of the TL). All other parameters have measures M_k and Σ_k close to 0 so that they are considered as unimportant parameters.

We would like to mention that the advantage of combining DGSM method with the adjoint state method is that the computation of measures M_k and Σ_k is independent from the number of uncertain parameters. For instance, if we would like to use the perturbation method to compute M_k and Σ_k, then we would need in total $r(N_p+1)$ calculations. The same number of calculations is also required for calculating the indices associated with the Morris screening method. However, only $2r$ calculations are needed using the adjoint state method.

6. Conclusion

In this paper, we presented the adjoint sensitivity model associated with the problem describing one-dimensional RN transport in heterogeneous porous media coupled with sequential first-order decay chain in a steady-state regime. Both continuous and discrete approaches were used to derive the adjoint state equations. For the continuous approach, the adjoint state partial differential equations and the sensitivity coefficients were formulated based on the adjoint state theory for coupled problems. For the discrete approach, the adjoint states are presented as solutions of matrix linear systems based on the discretized matrix system of the primary problem. A physical interpretation indicates that the adjoint state function associated with a given RN represents the rate at which the performance measure varies per unit source of RN.

For the case of a homogeneous porous medium, closed-form analytical solutions of the adjoint state systems associated with two performance measures are derived: combination of concentrations at a point of the finite domain and combination of integrated concentrations. The first performance measure could be used to represent the total concentration at a point (or the total advective flux at a point), while the second may be used to represent the total RN mass in the system at steady state. These closed-form adjoint states can be considered as reference solutions to validate other solutions obtained from numerical schemes. Sensitivity coefficients associated with three types of transport parameters are considered. The general analytical sensitivity coefficient formulas associated with each parameter are then presented as functions of the calculated concentrations and adjoint states. The adjoint state systems together with the primary systems are also solved numerically for both transport problems using MATLAB. Applications to the case of a three-member RN decay chain show excellent agreements between analytical and numerical adjoint states. The analytically calculated sensitivity coefficients are compared to numerical sensitivities obtained from the perturbation method based on the numerical solutions of the primary problems. The analytical and numerical sensitivities compare well to each other.

An inspectional analysis shows that the importance of a given parameter depends not only on its initial value but also on those of the other parameters. Therefore, a global sensitivity analysis is necessary to correctly identify the important parameters. In consequence, a derivative-based global sensitivity method coupled together with the adjoint state method is applied to a multilayer system representing a site currently being considered for underground nuclear storage in Northern Switzerland, Zürich Nordost, for identifying important/unimportant parameters with respect to the total RN flux leaving the system. Twelve parameters were considered including the effective diffusion coefficients and sorption coefficients of each layer. The results show that the most important parameters are four among them those associated with the host rock. The results show also the advantage of the adjoint state method compared to others screening methods such as the Morris method in term of computational effort.

Finally, it is important to note that, although the results presented here apply to the steady state case and can be readily extended to the time-dependent case, the latter has some unique feature that must be treated differently. The adjoint state sensitivity method applied to the transient case will be the subject of a forthcoming work.

Appendix A: Derivation of the Adjoint System

This appendix details the derivation of the adjoint system (11) and the associated boundary conditions (12) and (13) starting from equations (7)–(9).

The gradient operators $\nabla_{\mathbf{C}}\mathbf{L}$ and $\nabla_{\mathbf{p}}\mathbf{L}$ are defined as

$$\nabla_{\mathbf{C}}\mathbf{L}=\begin{bmatrix} \frac{\partial L_1}{\partial C_1} & \frac{\partial L_1}{\partial C_2} & \cdots & \frac{\partial L_1}{\partial C_N} \\ \frac{\partial L_2}{\partial C_1} & \frac{\partial L_2}{\partial C_2} & \cdots & \frac{\partial L_2}{\partial C_N} \\ \vdots & \vdots & \ddots & \vdots \\ \frac{\partial L_N}{\partial C_1} & \frac{\partial L_N}{\partial C_2} & \cdots & \frac{\partial L_N}{\partial C_N} \end{bmatrix}, \quad \nabla_{\mathbf{p}}\mathbf{L}=\begin{bmatrix} \frac{\partial L_1}{\partial p_1} & \frac{\partial L_1}{\partial p_2} & \cdots & \frac{\partial L_1}{\partial p_{N_p}} \\ \frac{\partial L_2}{\partial p_1} & \frac{\partial L_2}{\partial p_2} & \cdots & \frac{\partial L_2}{\partial p_{N_p}} \\ \vdots & \vdots & \ddots & \vdots \\ \frac{\partial L_N}{\partial p_1} & \frac{\partial L_N}{\partial p_2} & \cdots & \frac{\partial L_N}{\partial p_{N_p}} \end{bmatrix} \tag{A1}$$

The adjoint operators $\nabla^*_{\mathbf{C}}\mathbf{L}$ and $\nabla^*_{\mathbf{p}}\mathbf{L}$ are defined as the transpose adjoint operator matrices of $\nabla_{\mathbf{C}}\mathbf{L}$ and $\nabla_{\mathbf{p}}\mathbf{L}$:

$$\nabla^*_{\mathbf{C}}\mathbf{L}=\begin{bmatrix} \left[\frac{\partial L_1}{\partial C_1}\right]^* & \left[\frac{\partial L_2}{\partial C_1}\right]^* & \cdots & \left[\frac{\partial L_N}{\partial C_1}\right]^* \\ \left[\frac{\partial L_1}{\partial C_2}\right]^* & \left[\frac{\partial L_2}{\partial C_2}\right]^* & \cdots & \left[\frac{\partial L_N}{\partial C_2}\right]^* \\ \vdots & \vdots & \ddots & \vdots \\ \left[\frac{\partial L_1}{\partial C_N}\right]^* & \left[\frac{\partial L_2}{\partial C_N}\right]^* & \cdots & \left[\frac{\partial L_N}{\partial C_N}\right]^* \end{bmatrix}, \quad \nabla^*_{\mathbf{p}}\mathbf{L}=\begin{bmatrix} \left[\frac{\partial L_1}{\partial p_1}\right]^* & \left[\frac{\partial L_2}{\partial p_1}\right]^* & \cdots & \left[\frac{\partial L_N}{\partial p_1}\right]^* \\ \left[\frac{\partial L_1}{\partial p_2}\right]^* & \left[\frac{\partial L_2}{\partial p_2}\right]^* & \cdots & \left[\frac{\partial L_N}{\partial p_2}\right]^* \\ \vdots & \vdots & \ddots & \vdots \\ \left[\frac{\partial L_1}{\partial p_{N_p}}\right]^* & \left[\frac{\partial L_2}{\partial p_{N_p}}\right]^* & \cdots & \left[\frac{\partial L_N}{\partial p_{N_p}}\right]^* \end{bmatrix} \tag{A2}$$

where $[\partial L_i/\partial C_j]^*$ and $[\partial L_i/\partial p_j]^*$ are the adjoint operators of $\partial L_i/\partial C_j$ and $\partial L_i/\partial p_j$. Note that $\nabla_{\mathbf{C}}\mathbf{L}$ and $\nabla^*_{\mathbf{C}}\mathbf{L}$ are square matrices while $\nabla_{\mathbf{p}}\mathbf{L}$ and $\nabla^*_{\mathbf{p}}\mathbf{L}$ are not in general.

The elements of $\nabla_{\mathbf{C}}\mathbf{L}$ can be obtained by direct differentiation using (1). We obtain

$$\begin{cases} \frac{\partial L_i}{\partial C_i}=\frac{\mathrm{d}}{\mathrm{d}x}\left(D_i\frac{\mathrm{d}\cdot}{\mathrm{d}x}\right)-\frac{\mathrm{d}}{\mathrm{d}x}(V\cdot)-\phi k_i R_i \\ \frac{\partial L_i}{\partial C_{i-1}}=\phi k_{i-1}R_{i-1} \\ \frac{\partial L_i}{\partial C_j}=0, j\neq i-1, i \end{cases} \tag{A3}$$

Using the adjoint operation rule (Sun, 1994) for operator $\frac{\mathrm{d}}{\mathrm{d}x}$: $\left[\frac{\mathrm{d}}{\mathrm{d}x}\right]^* = -\frac{\mathrm{d}}{\mathrm{d}x}$, it follows from (A3):

$$\begin{cases} \left[\frac{\partial L_i}{\partial C_i}\right]^*=\frac{\mathrm{d}}{\mathrm{d}x}\left(D_i\frac{\mathrm{d}\cdot}{\mathrm{d}x}\right)+\frac{\mathrm{d}}{\mathrm{d}x}(V\cdot)-\phi k_i R_i \\ \left[\frac{\partial L_i}{\partial C_{i-1}}\right]^*=\phi k_{i-1}R_{i-1} \\ \left[\frac{\partial L_i}{\partial C_j}\right]^*=0, j\neq i-1, i \end{cases} \tag{A4}$$

Using (A4) and the definition of $\nabla^*_{\mathbf{C}}\mathbf{L}$ in (A2), we obtain the adjoint system of PDEs (11).

The boundary conditions (12) and (13) may be obtained as follows.

The first condition in equation (8) (i.e., $\boldsymbol{\lambda}=\mathbf{0}$) is used when a concentration boundary condition (2) is used for the primary Problem A, while the second condition (i.e., $\nabla^*_{\mathbf{C}}\mathbf{L}_{\mathbf{B}}\boldsymbol{\lambda}=\mathbf{0}$) corresponds to the primary Problem B with a flux boundary condition (3). For this latter case, the boundary operator $\mathbf{L}_{\mathbf{B}}$ is a N-dimensional vector with elements $L_{Bi}=-V(0)C_i(0)+D_i(0)\frac{\mathrm{d}C_i}{\mathrm{d}x}(0)$. Using the adjoint operation rules for the boundary operators (Sun, 1994), we can show that $\nabla^*_{\mathbf{C}}\mathbf{L}_{\mathbf{B}}$ is a diagonal matrix with all elements equal to $D_i\frac{\mathrm{d}\cdot}{\mathrm{d}x}\big|_{x=0}$. The boundary conditions (12) and (13) can be then easily deduced.

Appendix B: Exact Analytical Solutions of the Primary Problems

The analytical solutions for both primary and adjoint problems are derived by introducing the following dimensionless parameters:

$$X = \frac{x}{L}, \quad P_e = \frac{LV}{D}, \quad K_i = \frac{\phi L^2 k_i R_i}{D} \tag{B1}$$

where P_e is known as the Peclet number.

As mentioned in section 4, the exact solutions are obtained by applying the general method for solving multi-species coupled problems introduced by Clement (2001). Here we only present the exact solutions. The details of derivation can be found in the supporting information.

The exact solutions of the primary Problems A and B write for $i = 1,...,N$ and $0 \le X \le 1$ as follows:

$$C_i(X) = \widetilde{C}_i(X) + \sum_{j=1}^{i-1} \left(\prod_{l=j}^{i-1} \frac{K_l}{K_{l+1} - K_j} \right) \widetilde{C}_j(X) \tag{B2}$$

where $\widetilde{C}_i(X)$ defined by

$$\widetilde{C}_i(X) = \frac{\left[C_i^0 + \sum_{j=1}^{i-1} \left(\prod_{l=j}^{i-1} \frac{K_l}{K_l - K_i} \right) C_j^0 \right] e^{\frac{P_e}{2} X} \Phi_i(X)}{\Phi_i(0)} \tag{B3}$$

for Problem A, and

$$\widetilde{C}_i(X) = \frac{2L \left[F_i^0 + \sum_{j=1}^{i-1} \left(\prod_{l=j}^{i-1} \frac{K_l}{K_l - K_i} \right) F_j^0 \right] e^{\frac{P_e}{2} X} \Phi_i(X)}{D \left[P_e \Phi_i(0) + \sqrt{P_e^2 + 4K_i} \Psi_i(0) \right]} \tag{B4}$$

In equations (B3) and (B4), the functions $\Phi_i(X)$ and $\Psi_i(X)$ are defined by

$$\Phi_i(X) = \sinh\left[\frac{1}{2}(1-X)\sqrt{P_e^2 + 4K_i} \right], \quad \Psi_i(X) = \cosh\left[\frac{1}{2}(1-X)\sqrt{P_e^2 + 4K_i} \right] \tag{B5}$$

Appendix C: Exact Analytical Solutions of the Adjoint Problems

The exact solutions of the adjoint problems are derived for the performance measures defined by equations (25) and (26). In this appendix, we only provide the final solutions. The details of derivation can be found in the supporting information. The general form solution associated with both performance measures writes as follows:

$$\lambda_i(X) = \widetilde{\lambda}_i(X) + \sum_{j=i+1}^{N} \left(\prod_{l=i}^{j-1} \frac{K_l}{K_l - K_j} \right) \widetilde{\lambda}_j(X) \tag{C1}$$

where $\widetilde{\lambda}_i(X)$ depends on the performance measure type.

For the performance measure defined as a combination of RN concentrations at a point (i.e., equation (25)), $\widetilde{\lambda}_i(X)$ is a Green function, which is defined as follows.

For Problem A, the exact expression of $\widetilde{\lambda}_i(X)$ writes as follows: for $0 \le X \le X_0 = x_0/L$,

$$\widetilde{\lambda}_i(X) = \frac{2P_i e^{\frac{P_e}{2}(X_0 - X)} \Phi_i(X_0) \varphi_i(X)}{\sqrt{P_e^2 + 4K_i} \Phi_i(0)} \tag{C2}$$

and, for $X_0 \le X \le 1$,

$$\widetilde{\lambda}_i(X) = \frac{2P_i e^{\frac{P_e}{2}(X_0 - X)} \Phi_i(X) \varphi_i(X_0)}{\sqrt{P_e^2 + 4K_i}\Phi_i(0)} \tag{C3}$$

For Problem B, $\widetilde{\lambda}_i(X)$ is defined as follows:for $0 \le X \le X_0$,

$$\widetilde{\lambda}_i(X) = \frac{2P_i e^{\frac{P_e}{2}(X_0 - X)} \Phi_i(X_0) \left[P_e \varphi_i(X) + \sqrt{P_e^2 + 4K_i}\psi_i(X)\right]}{\sqrt{P_e^2 + 4K_i}\left[P_e \Phi_i(0) + \sqrt{P_e^2 + 4K_i}\Psi_i(0)\right]} \tag{C4}$$

and, for $X_0 \le X \le 1$,

$$\widetilde{\lambda}_i(X) = \frac{2P_i e^{\frac{P_e}{2}(X_0 - X)} \Phi_i(X) \left[P_e \varphi_i(X_0) + \sqrt{P_e^2 + 4K_i}\psi_i(X_0)\right]}{\sqrt{P_e^2 + 4K_i}\left[P_e \Phi_i(0) + \sqrt{P_e^2 + 4K_i}\Psi_i(0)\right]} \tag{C5}$$

with $P_i = L^2\left[\alpha_i + \sum_{j=i+1}^{N}\left(\prod_{l=i}^{j-1}\frac{K_l}{K_{l+1}-K_i}\right)\alpha_j\right]/D$ in equations (C2)–(C5).

For the performance measure defined as a combination of spatially integrated RN concentrations (i.e., equation (26)), the general analytical expression of $\widetilde{\lambda}_i(X)$ writes as follows:

$$\widetilde{\lambda}_i(X) = \frac{L^2}{DK_i}\left[\beta_i + \sum_{j=i+1}^{N}\left(\prod_{l=i}^{j-1}\frac{K_l}{K_{l+1}-K_i}\right)\beta_j\right]\left[1 - \frac{e^{-\frac{P_e}{2}X}\left[\Phi_i(X) + e^{\frac{P_e}{2}}\varphi_i(X)\right]}{\Phi_i(0)}\right] \tag{C6}$$

for Problem A, and

$$\widetilde{\lambda}_i(X) = \frac{L^2}{DK_i}\left[\beta_i + \sum_{j=i+1}^{N}\left(\prod_{l=i}^{j-1}\frac{K_l}{K_{l+1}-K_i}\right)\beta_j\right]\left[1 - \frac{e^{\frac{P_e}{2}(1-X)}\left[P_e\varphi_i(X) + \sqrt{P_e^2 + 4K_i}\psi_i(X)\right]}{P_e\Phi_i(0) + \sqrt{P_e^2 + 4K_i}\Psi_i(0)}\right] \tag{C7}$$

for Problem B.

In equations (C2)–(C8), the functions $\varphi_i(X)$ and $\psi_i(X)$ are defined by

$$\varphi_i(X) = \sinh\left(\frac{1}{2}X\sqrt{P_e^2 + 4K_i}\right), \quad \psi_i(X) = \cosh\left(\frac{1}{2}X\sqrt{P_e^2 + 4K_i}\right) \tag{C8}$$

Acknowledgments
Some of the data used in this study are synthetics, and the others can be found in Nagra (2014). We thank the anonymous reviewers for their thoughtful comments and suggestions.

References

Chavent, G. (2009). *Nonlinear least squares for inverse problems*. Dordrecht: Springer.

Clement, T. P. (2001). Generalized solution to multispecies transport equations coupled with a first-order reaction network. *Water Resources Research*, *37*(1), 157–163. https://doi.org/10.1029/2000WR900239

Clemo, T. (2007). MODFLOW-2005 Ground-water model-user guide to the adjoint state based sensitivity process, Tech. report BSU CGISS 07-01.

Delay, F., Badri, H., Fahs, M., & Ackerer, P. (2017). A comparison of discrete versus continuous adjoint states to invert groundwater flow in heterogeneous dual porosity systems. *Advances in Water Resources*, *110*, 1–18. https://doi.org/10.1016/j.advwatres.2017.09.022

de Marsily, G., Lavedan, G., Boucher, M., & Fasanio, G. (1984). Interpretation of interference tests in a well field using geostatistical techniques to fit the permeability distribution in a reservoir model. In G. Verly (Eds.), *Geostatistics for Natural Resources Characterization*, *NATO ASI Ser., Ser. C* (Vol. 122, part 2, pp. 831–849). Norwell, Massachusetts.

Fahs, H., Hayek, M., Fahs, M., & Younes, A. (2014). An efficient numerical model for hydrodynamic parameterization in 2D fractured dual-porosity media. *Advances in Water Resources*, *63*, 179–193. https://doi.org/10.1016/j.advwatres.2013.11.008

Hayek, M., Lehmann, F., & Ackerer, P. (2008). Adaptive multi-scale parameterization for one-dimensional flow in unsaturated porous media. *Advances in Water Resources*, *31*(1), 28–43. https://doi.org/10.1016/j.advwatres.2007.06.009

Kucherenko, S., Rodriguez-Fernandez, M., Pantelides, C., & Shah, N. (2009). Monte Carlo evaluation of derivative-based global sensitivity measures. *Reliability Engineering and System Safety*, *94*(7), 1135–1148. https://doi.org/10.1016/j.ress.2008.05.006

Larbkich, W., Neupauer, R., Colvin, D., Bauer, J., & Herman, J. (2014). Adjoint modeling of contaminant fate and transport in riverbank filtration systems. In W. C. Huber (Ed.), *World Environmental and Water Resources Congress 2014* (pp. 235–242). Va: Am. Soc. of Civ. Eng.

LaVenue, A. M., Andrews, R. W., & RamaRao, B. S. (1989). Groundwater travel time uncertainty analysis using sensitivity derivatives. *Water Resources Research*, *25*(7), 1551–1566. https://doi.org/10.1029/WR025i007p01551

LaVenue, A. M., RamaRao, B. S., de Marsily, G., & Mariette, M. G. (1995). Pilot point methodology for automated calibration of an ensemble of conditionally simulated transmissivity fields. 2. Application. *Water Resources Research*, *31*(3), 495–516. https://doi.org/10.1029/94WR02259

Li, B., & Yeh, T.-C. J. (1998). Sensitivity and moment analyses of head in variably saturated regimes. *Advances in Water Resources*, *21*(6), 477–485. https://doi.org/10.1016/S0309-1708(97)00011-0

Lu, Z., & Vesselinov, V. V. (2015). Analytical sensitivity analysis of transient groundwater flow in a bounded model domain using the adjoint method. *Water Resources Research*, *51*, 5060–5080. https://doi.org/10.1002/2014WR016819

Michalak, A. M., & Kitanidis, P. K. (2004). Estimation of historical groundwater contaminant distribution using the adjoint state method applied to geostatistical inverse modeling. *Water Resources Research*, *40*, W08302. https://doi.org/10.1029/2004WR003214

Morris, M. (1991). Factorial sampling plans for preliminary computational experiments. *Technometrics*, *33*(2), 161–174. https://doi.org/10.1080/00401706.1991.10484804

Nagra (2014). SGT Etappe 2: Vorschlag weiter zu untersuchender geologischer Standortgebiete mit zugehörigen Standortarealen für die Oberflächenanlage: Charakteristische Dosisintervalle und Unterlagen zur Bewertung der Barrierensysteme. Nagra Tech. Rep. NTB 14-03. December 2014, Wettingen, Switzerland.

Neupauer, R. M., & Wilson, J. L. (1999). Adjoint method for obtaining backward-in-time location and travel time probabilities of a conservative groundwater contaminant. *Water Resources Research*, *35*(11), 3389–3398. https://doi.org/10.1029/1999WR900190

Neupauer, R. M., & Wilson, J. L. (2001). Adjoint-derived location and travel time probabilities for a multidimensional groundwater system. *Water Resources Research*, *37*(6), 1657–1668. https://doi.org/10.1029/2000WR900388

Piasecki, M., & Katopodes, N. D. (1997). Control of contaminant releases in rivers. I: Adjoint sensitivity analysis. *Journal of Hydraulic Engineering*, *123*(6), 486–492. https://doi.org/10.1061/(ASCE)0733-9429(1997)123:6(486)

RamaRao, B. S., Kelley, V. A., & Lavenue, M. (2017). Capture functions in a coupled surface water-groundwater model using MODFLOW-ADJOINT Code, *Modeling for sustainability and adaptation, Proceedings of the MODFLOW and More 2017 Conference May 21-24, 2017*, Golden, Colorado.

RamaRao, B. S., LaVenue, A. M., de Marsily, G., & Mariette, M. G. (1995). Pilot point methodology for automated calibration of an ensemble of conditionally simulated transmissivity fields. 1. Theory and computational experiments. *Water Resources Research*, *31*(3), 475–493. https://doi.org/10.1029/94WR02258

RamaRao, B. S., & Mishra, S. (1996). Adjoint sensitivity analysis for mathematical models of coupled nonlinear physical process. In *Calibration and Reliability in Groundwater Modelling*, *Proceedings of the ModelCARE 96 Conference* (Vol. 237, pp. 483–490). Golden, Colorado: IAHS Publ.

Samper, F. J., & Neuman, S. P. (1986). Adjoint state equations for advective-dispersive transport. In A. Sa da Costa, A. M. Baptista, W. G. Gray, C. A. Brebbia, & G. F. Pinder (Eds.), *Finite elements in water resources, Proceedings of the 6th International Conference* (pp. 423–438). Southampton/Berlin: Computational Mechanics Publications/Springer Verlag.

SFOE (2008). Sectoral plan for deep geological repositories—Conceptual part. Department of Environment, Transport, Energy and Communications (DETEC)/SFOE. April 2008, Bern, Switzerland.

Sobol, I. M. (1976). Uniformly distributed sequences with an additional uniform property. *USSR Computational Mathematics and Mathematical Physics*, *16*(5), 236–242. https://doi.org/10.1016/0041-5553(76)90154-3

Sobol, I. M. (1993). Sensitivity estimates for nonlinear mathematical models. *MMCE*, *1*(4), 407–414.

Sobol, I. M. (1998). On quasi-Monte Carlo integrations. *Mathematics and Computers in Simulation*, *47*(2-5), 103–112. https://doi.org/10.1016/S0378-4754(98)00096-2

Sun, N. Z. (1994). *Inverse problems in groundwater modeling*. Massachusetts: Kluwer.

Sykes, J. F., Wilson, J. L., & Andrews, R. W. (1985). Sensitivity analysis for steady state groundwater flow using adjoint operators. *Water Resources Research*, *21*(3), 359–371. https://doi.org/10.1029/WR021i003p00359

Wilson, J. L., & Metcalfe, D. E. (1985). Illustration and verification of adjoint sensitivity theory for steady state groundwater flow. *Water Resources Research*, *21*(11), 1602–1610. https://doi.org/10.1029/WR021i011p01602

Yeh, W. W.-G. (1986). Review of parameter identification procedures in groundwater hydrology: The inverse problem. *Water Resources Research*, *22*(2), 95–108. https://doi.org/10.1029/WR022i002p00095

Erratum

In the originally published version of this article, Equation 34 was typeset incorrectly. The equation has since been corrected and this version may be considered the authoritative version of record.